

Distinguishing zero-group-velocity modes in photonic crystals

M. Ghebregbrhan, M. Ibanescu, Steven G. Johnson, M. Soljačić, and J. D. Joannopoulos

Department of Physics, Massachusetts Institute of Technology, 77 Massachusetts Avenue, Cambridge, Massachusetts 02139, USA

(Received 28 August 2007; published 14 December 2007)

We examine differences between various zero-group-velocity modes in photonic crystals, including those that arise from Bragg diffraction, anticrossings, and band repulsion. Zero-group velocity occurs at points where the group velocity changes sign, and therefore is conceptually related to “left-handed” media, in which the group velocity is opposite to the phase velocity. We consider this relationship more quantitatively in terms of the Fourier decomposition of the modes, by defining a measure of how much the “average” phase velocity is parallel to the group velocity—an anomalous region is one in which they are mostly antiparallel. We find that this quantity can be used to qualitatively distinguish different zero-group-velocity points. In one dimension, such anomalous regions are found never to occur. In higher dimensions, they are exhibited around certain zero-group-velocity points, and lead to unusual enhanced confinement behavior in microcavities.

DOI: [10.1103/PhysRevA.76.063810](https://doi.org/10.1103/PhysRevA.76.063810)

PACS number(s): 42.70.Qs

Photonic crystals are periodic dielectric and metallo-dielectric media [1–3] in which the propagation of light can exhibit behaviors quite different from those of homogeneous media—behaviors such as photonic band gaps, supercollimation, superprism effects [4], and extraordinary or negative refraction [5]. Most of these effects are closely associated with an unusual feature of the dispersion relation (band structure), the frequency ω versus wave vector \mathbf{k} , of periodic systems: There are extrema, or points of zero-group velocity $d\omega/d\mathbf{k}$. Such points do not occur in a homogeneous medium, only in localized modes of certain waveguide structures or in nonlocalized modes of periodic media. Since extrema in the frequency bands are so central to the unique phenomena possible in photonic crystals, we wish to investigate them more closely, and to ask the following question: Are there significant qualitative differences between different band extrema, and what relationship do these differences have to various physical phenomena? Naturally, there are some obvious qualitative differences: Some extrema are maxima, some are minima, and others are saddle points. Of course, the exact eigenmode solutions in the vicinity of the extrema provide, in principle, complete information about their behavior. But the latter is too much information—we would hope to have a simpler description of the differences between extrema than the entire field patterns—and the former is too little, as we shall see. In particular, we will argue that there are substantial differences between extrema at high-symmetry \mathbf{k} points (such as the center or edge of the Brillouin zone, corresponding to the traditional criteria for Bragg diffraction) and extrema at other \mathbf{k} . Even among these nonsymmetric extrema, there are distinct differences between those arising from avoided eigenvalue crossings (anticrossings) and other band-repulsion phenomena. As we will show these differences arise from general properties of periodic crystals, therefore such differences in zero-group velocity should be found in other periodic systems, including electronic and phononic crystals.

In order to have a quantitative measure of these differences independent of any particular physical phenomena, we consider by analogy an important quantity of homogeneous media that is ill-defined in periodic structures: the phase velocity $\mathbf{v}_p = \omega\mathbf{k}/|\mathbf{k}|^2$. In a homogeneous medium, the relative

direction of the phase and group velocities reveals important information such as whether the medium is right- or left-handed (negative index) [6] and to what degree the medium is isotropic. In a periodic medium, the phase velocity is ill-defined because \mathbf{k} is not unique—it is equivalent to $\mathbf{k} + \mathbf{G}$ for any reciprocal lattice vector \mathbf{G} [1]. Equivalently, an eigenmode in a periodic structure corresponds to an infinite number of Fourier components $\mathbf{k} + \mathbf{G}$, given by the Fourier-series expansion of the Bloch envelope, each with its own “phase velocity.” However, we can use the amplitudes of these Fourier components, $\mathbf{H}_{\mathbf{k}+\mathbf{G}}$, to quantify the degree to which the solution resembles that of a homogeneous medium and the degree to which the “average” phase velocity is parallel to the group velocity, and we find that this average exhibits interesting distinctions between different band extrema. In particular, we define

$$\eta_{\mathbf{H}} = \frac{\sum_{\mathbf{G}} \frac{\mathbf{v}_g \cdot (\mathbf{k} + \mathbf{G})}{|\mathbf{v}_g| |\mathbf{k} + \mathbf{G}|} |\mathbf{H}_{\mathbf{k}+\mathbf{G}}|^2}{\sum_{\mathbf{G}} |\mathbf{H}_{\mathbf{k}+\mathbf{G}}|^2} \quad (1)$$

as a measure of the anomalous character of a mode. As a sum of cosines of the angle between the group velocity and the wave vector weighted by the Fourier component amplitude, $\eta_{\mathbf{H}}$ is bounded between -1 and 1 . A positive (negative) sign indicates normal (anomalous) character; in fact in the homogeneous, right-handed medium limit $\eta_{\mathbf{H}}$ is 1 for all modes. The form of this function is somewhat arbitrary, e.g., one could just as easily use the electric field instead of the magnetic field, but as we will see later, alternative definitions of η yield similar qualitative results.

Consider a one-dimensional photonic crystal, such as a multilayer film of period a with alternating $\varepsilon=9$ (thickness $0.2a$) and $\varepsilon=1$ (thickness $0.8a$), whose band structure $\omega(k)$ (solved using a plane-wave method [7]) is shown in Fig. 1. In such a structure, there are bands that have opposite-signed group velocity and k , and which therefore appear “anomalous,” but examining $\eta_{\mathbf{H}}$, Fig. 2(a), reveals that they are not. The first band is the only band in which $\eta_{\mathbf{H}}$ approaches a constant nonzero value as k vanishes, behavior due to the

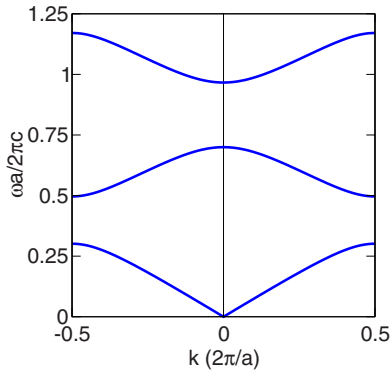


FIG. 1. (Color online) Typical one-dimensional band structure for a Bragg mirror with $\epsilon=9$ and width of high dielectric layer $d=0.2a$.

fact that v_g approaches a constant nonzero value at low frequencies. The second band, which looks anomalous since v_g is opposite to k in the first Brillouin zone, is shown to be “normal” in the sense of η_H : Most of its Fourier components actually lie at negative wave vectors, aligned with v_g . Since all other bands have the behavior of one of these two bands, it appears that all one-dimensional modes have similar, normal character.

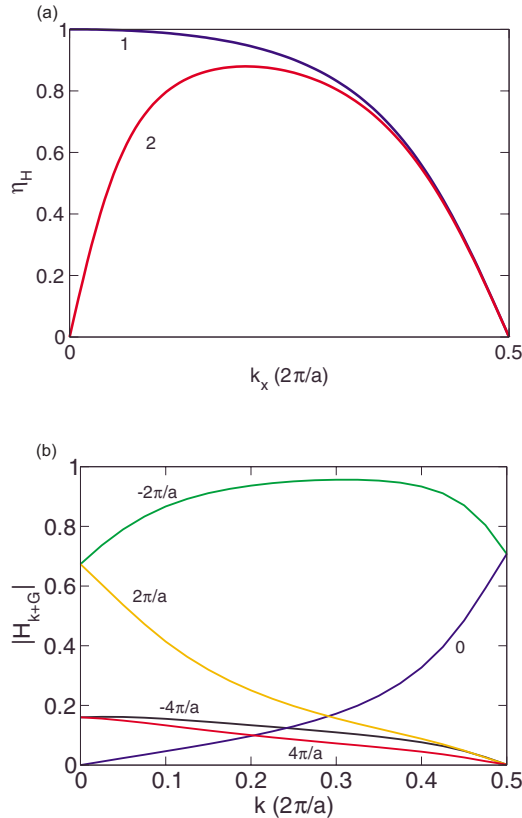


FIG. 2. (Color online) (a) η_H calculated across the first and second bands is never negative. (b) The strengths of the most important Fourier components for the second band of Fig 1. Away from the band edges, where strong mixing occurs, the second band behaves as a plane wave with $k=k-2\pi/a$.

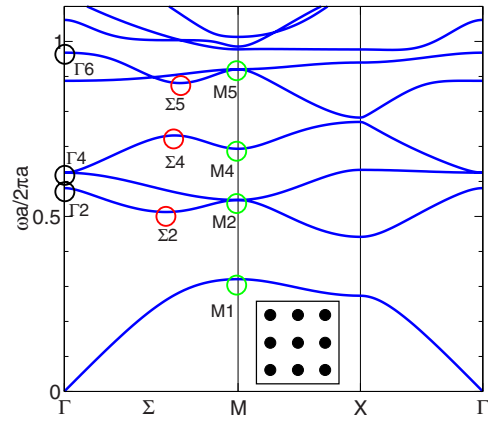


FIG. 3. (Color online) 2D band structure with dielectric profile (inset) $\epsilon=9$, $r=0.2a$. Circled are the different types of zero-group-velocity points; the labels indicate location in the irreducible Brillouin zone and band number. Strong repulsion also creates a pronounced anticrossing in the fourth and fifth bands.

Fourier decomposing the modes of the second band shows the lack of any anomalous character more explicitly. In Fig. 2(b) the various Fourier components of the second band are plotted. The Fourier component $G=-2\pi/a$ is over 60% for most of the Bloch modes between $k=0$ and π/a . Effectively the mode at k acts like mostly a plane wave at $k-2\pi/a$. The group velocity and the “average” k point in the same direction. For vanishing k , the modes begin to have an additional mirror symmetry plane, so for every G there is a $-G$ component that cancels its contribution to η_H ensuring that η_H goes to zero.

There is a simple argument why one-dimensional photonic crystals should not exhibit sign changes of η_H , and therefore should not exhibit negative η_H for right-handed materials. To begin with, for a given frequency ω , the allowed wave vectors k in a one-dimensional crystal come from the eigenvalues $\exp(ika)$ of a 2×2 transfer matrix [8], and thus there can be at most two distinct real- k solutions at each ω . This precludes the possibility of having more than two extrema in a given band, and by symmetry (either mirror symmetry or time-reversal symmetry) these two extrema must occur at the Brillouin-zone edges. By the same symmetry, however, η_H cannot change sign at these points. The only remaining possibility would be for η_H to change sign at a point that is not an extremum, where v_g does not change sign, but this seems unlikely and we have been unable to find such a circumstance.

For two-dimensional periodic structures there can be zero-group-velocity modes away from the Brillouin-zone edge or center. For example, a square lattice (period a) of dielectric ($\epsilon=9$) rods (radius $r=0.2a$) in air illustrates this new type of zero-group-velocity mode at $\mathbf{k}=\Sigma$ where Σ lies on ΓM (Fig. 3), which itself can be divided into further subcategories. Around the M point, repulsion occurs between the second and fourth bands that causes the second band to develop a local minimum, where we might hope to find unusual behavior compared to a homogeneous right-handed medium. The repulsion that drives the second band downward originates in the shared symmetry character of the sec-

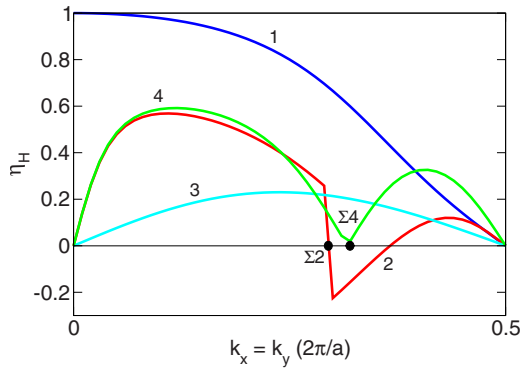


FIG. 4. (Color online) Plot of η_H for the first four bands of the two-dimensional crystal in Fig. 3.

ond and fourth bands under reflection about the mirror plane that contains \mathbf{k} along ΓM . Perturbative analysis of the modes near M of the second band, by expanding them in the basis of the eigenmodes at M , shows that the second band is indeed composed partly of the fourth mode at M [9]. Another type of zero-group-velocity mode is due to the avoided crossing along a high symmetry direction in bands four and five. The difference between these two types of extrema, both located away from the Brillouin-zone edge or center, is evident in η_H , shown in Fig. 4. A small region in the second band has negative η_H (which grows if we increase ε to increase the repulsion between the second and fourth bands). In contrast, the anticrossing in the fourth band does not produce a negative η_H , though it is responsible for the dip in η_H . The third band shows that “negative” group velocity (opposite to k in the first Brillouin zone) does not imply negative η_H .

A look at the amplitudes of the Fourier components, Fig. 5(a), explains the behavior of the second band. Along the second band, one pair of modes dominate for most of the band, and even when the “positive phase velocity” $\mathbf{G}/2\pi = (0,0)$ component increases in value the “negative phase velocity” $\mathbf{G}/2\pi = (-1,-1)$ component initially compensates for it. This allows the “average phase velocity” to remain negative and hence allows η_H to become negative just after the minimum. For comparison, the third band where the group velocity is always “negative” in this range of k has a Fourier decomposition that is always dominated by one pair of “negative phase velocity” components.

It should be emphasized that the sign of η_H does not determine whether there is negative or positive refraction at a (11) interface of the structure. The direction of refraction is not determined by the dominant Fourier decomposition, but essentially by whether the mode has any $\mathbf{G}=0$ Fourier component that an incident wave from a homogeneous medium can couple to at the given Bloch wave vector. Thus, “left-handedness” is not strictly required for negative refraction. For example, in this structure, the first two bands are negative refracting near M with a positive η_H , similar to the structure considered in Ref. [10]. As another example, the negative-refracting modes looked at in Ref. [5], the entire first band is dominated by the $\mathbf{G}=0$ component, yielding a positive η_H . (Of course, one can define an “effective index” by arbitrarily choosing a phase velocity from \mathbf{k} in the first

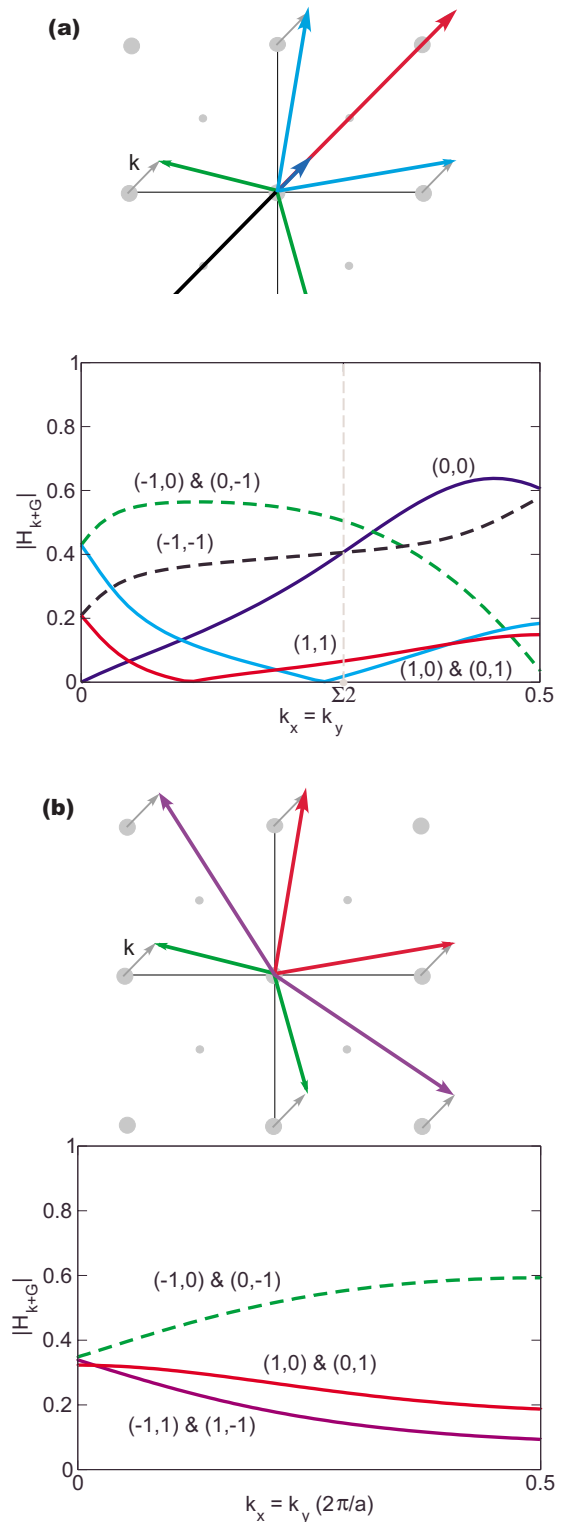


FIG. 5. (Color online) (a) A plot in k space of $\mathbf{k}+\mathbf{G}$ associated with the largest Fourier components for the second band. Below is a graph of the associated Fourier components across the same band (b) Corresponding graphs for the third band.

Brillouin zone [5,10], but this need not coincide with the average phase velocity determined by the Fourier decomposition.) Uniform cross-section waveguides (in which phase velocity is well defined) with group velocity opposite to

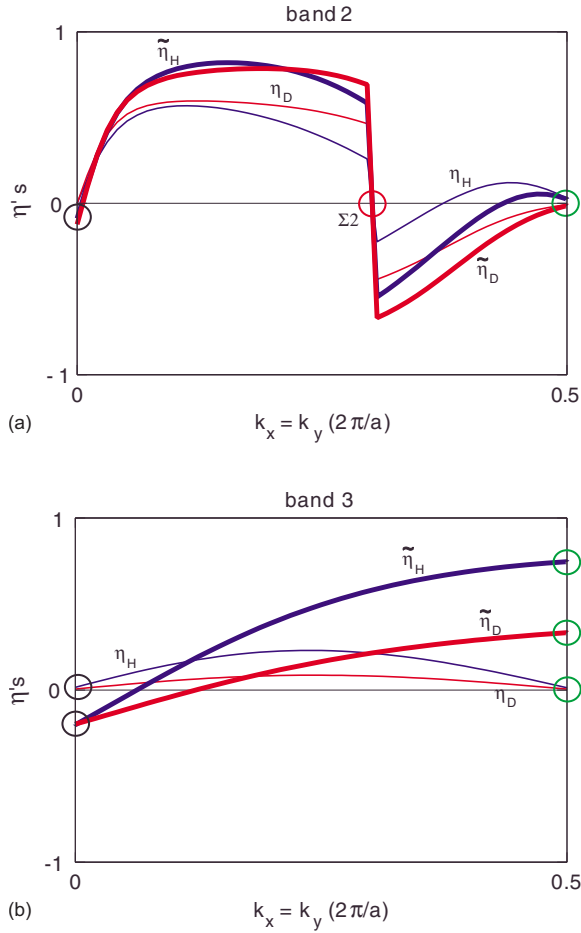


FIG. 6. (Color online) (a) Plot of η (thin lines) and $\tilde{\eta}$ (thick lines) for the second band. Color indicates the field used as the weight: \mathbf{H} (blue) and \mathbf{D} (red). (b) Same comparison but for the third band where behavior is expected to be normal.

phase velocity (and hence $\eta < 0$) have also been identified [11]. However, at any given frequency in these waveguides there are always both negative- and positive- η modes, whereas in the crystal considered here it is possible to get only $\eta < 0$ modes in a certain frequency range by tuning the rod radius.

To ensure that the behavior exhibited by $\eta_{\mathbf{H}}$ is not an artifact of some arbitrary choice in our definition, we explored other definitions and verified that the qualitative results do not change. For example, one can define $\eta_{\mathbf{D}}$ by simply replacing \mathbf{H} with \mathbf{D} , the electric displacement field, in Eq. (1). One can also define $\tilde{\eta}_{\mathbf{H}}$, the difference between the Fourier components with $\mathbf{k} + \mathbf{G}$ making acute angles with \mathbf{v}_g and those with obtuse angles.

$$\tilde{\eta}_{\mathbf{H}} = \sum_{\mathbf{G}}^{\mathbf{(k+G)} \cdot \mathbf{v}_g \geq 0} |\mathbf{H}_{\mathbf{k+G}}|^2 - \sum_{\mathbf{G}}^{\mathbf{(k+G)} \cdot \mathbf{v}_g < 0} |\mathbf{H}_{\mathbf{k+G}}|^2. \quad (2)$$

A corresponding quantity $\tilde{\eta}_{\mathbf{D}}$ using the Fourier components of \mathbf{D} can also be defined. Figures 6(a) and 6(b) plot these alternative definitions, compared with $\eta_{\mathbf{H}}$, for bands two and three, and show that the qualitative behavior around the zero-group-velocity point is preserved. The $\tilde{\eta}$ definitions do be-

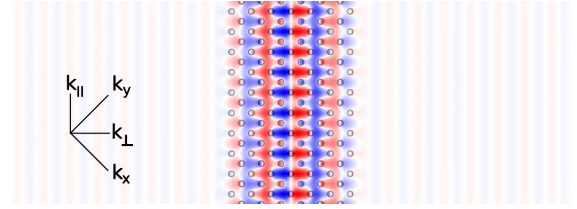


FIG. 7. (Color online) Photonic-crystal Fabry-Perot cavity, formed by a finite number of layers of the crystal in the (11) direction. Here, the thickness is $L = 12d$, where $d = a/\sqrt{2}$ is the distance from one layer to the next. (Blue, white, red) indicate (positive/zero/negative) E_z field of a resonant mode with $Q \sim 2000$.

come negative near Γ , but this is an artifact of them weighting the Fourier components that are only slightly on the “positive” side, such as $\mathbf{G}a/2\pi = (1, -1)$ and $(-1, 1)$, equally with very positive Fourier components such as $\mathbf{G}a/2\pi = (1, 0)$ or $(1, 1)$, rather than weighting them with the dot product $\mathbf{v}_g \cdot (\mathbf{k} + \mathbf{G})$. (Similarly for the fact that the third band has nonzero $\tilde{\eta}$ at the M point.)

One manifestation of the differences between the zero-group-velocity modes can be found in the dependence of cavity quality factors on the cavity length. Here, we are considering the simplest one-dimensional realization of an optical cavity: A slab of some material (or crystal structure) terminated by two mirrors on either end, which confines standing wave modes that leak out slowly due the imperfect reflectivity of the ends. Even simpler, we can omit the mirrors and just rely on the innate reflectivity of the interface between the cavity material or structure and the surrounding material (e.g., air). The quality factor Q is a conventional dimensionless lifetime (the number of optical periods for the energy to decay by $e^{-2\pi}$). Normally, the quality factor increases monotonically as the size of a cavity is increased, all other things equal, simply because a smaller portion of the mode is exposed to the edge of the cavity where it can escape (or equivalently because the round-trip time through the cavity increases). However, if the cavity material has a band extremum, more unusual length dependence can occur at frequencies near this extremum. Given the wave vector \mathbf{k} of the extremum, the component k_{\perp} perpendicular to the cavity interfaces introduces a length scale π/k_{\perp} , and as the cavity length changes by multiples of this length scale there are interference effects that lead to periodic peaks in Q [12]. If the extremum occurs in a periodic medium, however, there are multiple length scales corresponding to the different Fourier components $\mathbf{k} + \mathbf{G}$ (unless one component dominates), and the phenomena are more complicated. Moreover, in a periodic medium the thickness of the cavity cannot be increased continuously without changing the crystal termination, and so at best one expects periodic peaks in Q at the least common multiple of π/k_{\perp} and the crystal period.

In particular, we consider structures like the one depicted in Fig. 7: a finite number of layers of our square-lattice 2D crystal, oriented in the diagonal (11) direction, with thickness L in units of $d = a/\sqrt{2}$ (the distance from one layer to the next along the diagonal direction). This structure is periodic along the vertical ($\bar{1}\bar{1}$) direction, and so the modes would be characterized by a k_{\parallel} Bloch wave vector along this direction (par-

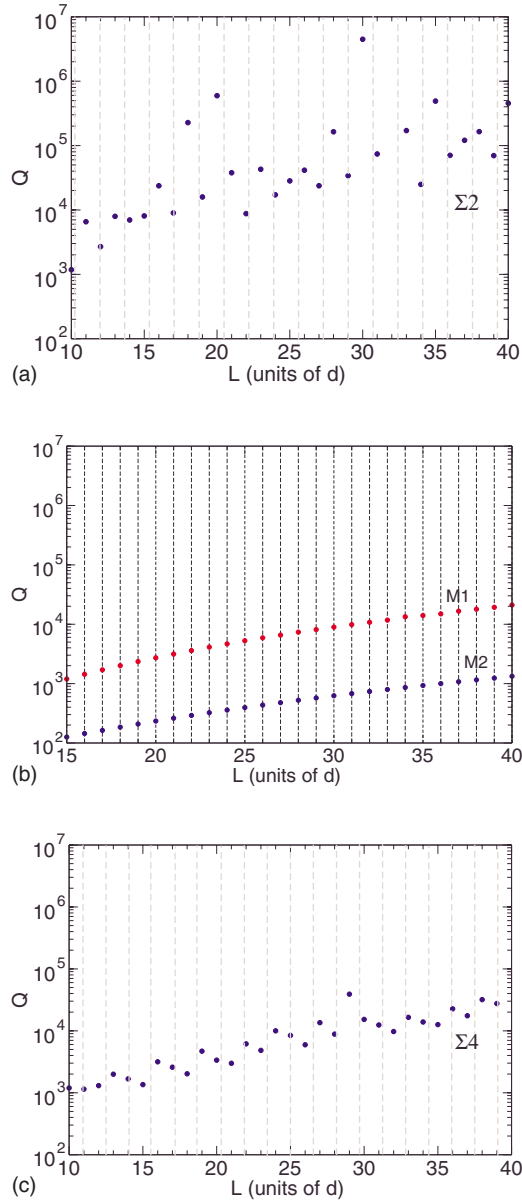


FIG. 8. (Color online) Resonant modes of a cavity formed from a finite section of a photonic crystal. The unit of length is $d = a/\sqrt{2}$ where a is the lattice constant. The dashed gray lines mark the induced periodicity due to the k point with zero-group velocity. For (a) $\mathbf{k}=(2\pi/a)(0.293,0.293)$ at $\Sigma 2$, (b) $\mathbf{k}=(2\pi/a)(0.5,0.5)$ at $M1$ and $M2$, and (c) $\mathbf{k}=(2\pi/a)(0.318,0.318)$ at $\Sigma 4$.

allel to the cavity interfaces), but we only consider $k_{\parallel}=0$ modes (which couple to normal-incident radiation). Even for $k_{\parallel}=0$, there are many resonant standing-wave modes at different frequencies, associated with different zero-group-velocity band edges along the ΓM direction. One such mode, at a frequency corresponding to the $\Sigma 2$ extremum of the second band, is depicted in Fig. 7 for $L=12d$.

We then compute the Q of modes associated with four different band extrema as a function of the cavity size L , and plot the results in Figs. 8(a)–8(c). (Q is computed using a filter-diagonalization analysis [13] of a finite-difference time-domain simulation [14] implemented in a free software package [15].) In each one of these plots, as discussed above, we

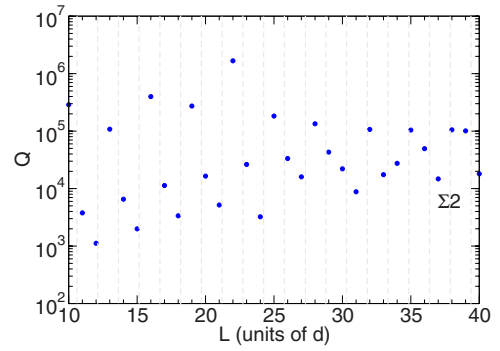


FIG. 9. (Color online) Shifting the second band minimum to occur at $\mathbf{k}=(2\pi/a)(0.33,0.33)$ yields the same oscillatory dependence on L shown in the fourth band in Fig. 8(c).

might expect to see periodic peaks in Q at intervals $\Delta L = \pi/k_{\perp}$, but this will be complicated by the periodicity of the underlying structure (and the corresponding nonuniqueness of \mathbf{k}). The simplest behavior occurs for the band extrema $M1$ and $M2$ at the M point $\mathbf{k}a/2\pi=(0.5,0.5)$, for which $k_{\perp} = \pi/d$. In this case, since the primary length scale (corresponding to the largest Fourier component $\mathbf{G}=0$) induces a length scale $\pi/k_{\perp}=d$ equal to the increment in L , the graphs appear smooth and monotonically increasing as expected from above. The most interesting results are shown in Fig. 8(a) corresponding to the $\Sigma 2$ extremum [$\mathbf{k}a/2\pi=(0.293,0.293)$], for which Q exhibits dramatic spikes (increasing by up to two orders of magnitude to $Q \sim 10^6$) at apparently irregular intervals. The ability of $\Sigma 2$ modes to exhibit extremely large Q compared to other band extrema lies in interference between the four modes in the crystal around such an extremum, as discussed further below. The irregularity of the peaks lies in the fact that the induced length scale $\pi/k_{\perp}=d/0.586$ does not have a small least-common multiple with d . In contrast, consider Fig. 8(c), which comes from the $\Sigma 4$ anticrossing extremum at $\mathbf{k}a/2\pi=(0.318,0.318)$, which has an induced length scale π/k_{\perp} that is close to $3d/2$, and hence Q displays nearly periodic peaks with period $3d$. The peaks in this case are not nearly so large as for Fig. 8(a), as discussed below, because the distinctness of the modes surrounding the extremum inhibits interference effects. To further reinforce our understanding of the Q peaks in Fig. 8(a), verifying that they indeed stem from an interference effect associated with \mathbf{k} at the extremum, we examined a slightly modified structure: We tweaked the index contrast to shift the $\Sigma 2$ extremum to $\mathbf{k}a/2\pi=(0.33,0.33)$. In this case, the induced length scale of the dominant Fourier component is $\pi/k_{\perp} \approx 3d/2$, and we expect to see periodic Q peaks at intervals of roughly $3d$. This prediction is confirmed in Fig. 9, which displays Q vs L for this tweaked structure. (Q is still not exactly periodic because there are multiple \mathbf{G} components present, but the largest peaks are separated by $\Delta L=3d$.)

The unusual behavior of the cavity Q in Fig. 8(a), with its many sharp peaks, lies in an interference phenomenon: as shown in Fig. 10, near a band extremum away from the edge of the Brillouin zone we have four modes out of which to build a standing-wave resonance, instead of only two modes

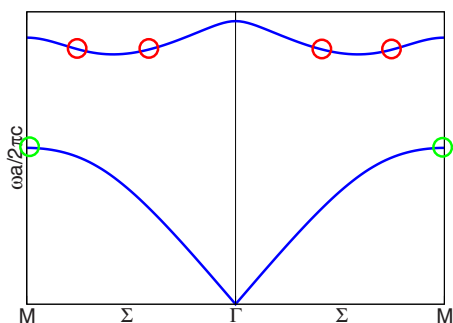


FIG. 10. (Color online) Differences in the number of excited modes for the two cases in Figs. 8(a) and 8(b).

as for an ordinary extremum at the zone edge or center. These four modes, or two pairs of counterpropagating modes, can form a superposition of two standing-wave patterns whose radiative fields destructively interfere, thus increasing Q . This can happen for both the extremum of the second band, where $\eta_{\mathbf{H}}$ changes sign, and for the extremum of the fourth band, where $\eta_{\mathbf{H}}$ does not change sign. But as shown in Fig. 8(a) the former have much more pronounced peaks in Q than the latter. This difference is directly connected to the change of sign in $\eta_{\mathbf{H}}$. As a general principle, one expects that modes that are more similar will interfere more readily, and hence have larger Q peaks. Perhaps counterintuitively, the fact that $\eta_{\mathbf{H}}$ changes sign, is an indication

that modes just on either side of the extremum in the second band are more similar than the corresponding modes for the fourth band where $\eta_{\mathbf{H}}$ does not change sign. The reason for this is that $\eta_{\mathbf{H}}$ changes sign only when the Fourier decomposition of the field pattern is similar (and hence has a similar “phase velocity”) on either side of the extremum despite the change in sign of the group velocity. Hence, the change in sign of $\eta_{\mathbf{H}}$ is correlated to the higher Q peaks for the second band.

In conclusion, it has been shown that a new measure of anomalous behavior, $\eta_{\mathbf{H}}$ determined by the average phase velocity, which was motivated by homogeneous negative-index media, can yield new information differentiating among the zero-group-velocity modes. This characterization of anomalous behavior appears to be independent of the arbitrary choice of norm used to define “average” phase velocity. Zero-group-velocity modes away from high-symmetry points exhibit qualitatively different behavior than zero-group-velocity modes at the band edge, and even among themselves have distinct behaviors depending on the sign of $\eta_{\mathbf{H}}$.

This work was supported in part by the Materials Research Science and Engineering Center Program of the National Science Foundation under Grant No. DMR 02-13282 and the Institute for Soldier Nanotechnologies under Contract No. DAAD-19-02-D0002.

-
- [1] J. D. Joannopoulos, R. D. Meade, and J. N. Winn, *Photonic Crystals: Molding the Flow of Light* (Princeton University Press, Princeton, NJ, 1995).
 - [2] E. Yablonovitch, *Phys. Rev. Lett.* **58**, 2059 (1987).
 - [3] S. John, *Phys. Rev. Lett.* **58**, 2486 (1987).
 - [4] H. Kosaka, T. Kawashima, A. Tomita, M. Notomi, T. Tamamura, T. Sato, and S. Kawakami, *Appl. Phys. Lett.* **74**, 1212 (1999).
 - [5] C. Luo, S. G. Johnson, J. D. Joannopoulos, and J. B. Pendry, *Phys. Rev. B* **65**, 201104(R) (2002).
 - [6] V. G. Veselago, *Sov. Phys. Usp.* **10**, 509 (1968).
 - [7] S. G. Johnson and J. D. Joannopoulos, *Opt. Express* **8**, 173 (2001).
 - [8] P. Yeh, *Optical Waves in Layered Media* (Wiley, New York, 1988).
 - [9] J. E. Sipe, *Phys. Rev. E* **62**, 5672 (2000).
 - [10] M. Notomi, *Phys. Rev. B* **62**, 10696 (2000).
 - [11] M. Ibanescu, S. G. Johnson, D. Roundy, C. Luo, Y. Fink, and J. D. Joannopoulos, *Phys. Rev. Lett.* **92**, 063903 (2004).
 - [12] M. Ibanescu, S. G. Johnson, D. Roundy, Y. Fink, and J. D. Joannopoulos, *Opt. Lett.* **30**, 552 (2005).
 - [13] V. A. Mandelshtam and H. S. Taylor, *J. Chem. Phys.* **107**, 6756 (1997).
 - [14] A. Taflov and S. C. Hagness, *Computational Electrodynamics: The Finite-Difference Time-Domain Method* (Artech, Norwood, MA, 2000).
 - [15] A. Farjadpour, D. Roundy, A. Rodriguez, M. Ibanescu, P. Bermeil, J. D. Joannopoulos, S. G. Johnson, and G. W. Burr, *Opt. Lett.* **31**, 2972 (2006).